厚生労働科学研究費補助金

こころの健康科学研究事業

ナンセンス変異型筋ジストロフィーの リードスルー薬物による治療法の確立

平成17年度　総括・分担研究報告書

主任研究者　松田　良一

平成18（2006）年　4月

目次

はじめに

筋ジストロフィーは遺伝子病の治療手段として正常な遺伝子の導入が有効であると考えられる。しかし、アデノウイルスベクターの持つ炎症惹起作用とともにジストロフィンのようにベクターの容量を超えて巨大な場合（cDNAは14kb）には最適とはいいがたい。また、幹細胞の移植も試みられているが、移植した細胞による腫瘍形成の問題や半致死量の放射線を照射したレシピエントマウスとヒト患者を同等に考えることは難しいなど解決すべき課題は多い。一方、遺伝子発現を制御する薬物療法も期待されている。特に1999年に初めて報告されたゲンタマイシンの持つストップコドンの読み越え（リードスルー）活性を利用した筋ジストロフィーマウス（mdx）のジストロフィン復活実験は遺伝子導入や幹細胞移植に次ぐ第三の戦略として注目された。しかし、そのようなリードスルー惹起物質の検索手段、物質の投与ルート、投与量なとの最適化をおこなう実験系の開発は進んでおらず、副作用が憂慮されるゲンタマイシンしか適用されていないのが現状である。一方、リードスルーそれ自体の分子機構はほとんど分かっておらず、長期間投与の副作用についても不明である。

我々は、未承認抗生物質ネガマイシンがマウス骨格筋に対してリードスルー活性を持つことを示してきた。本研究「ナンセンス変異型筋ジストロフィーのリードスルー薬物による治療法の確立」において、平成１７年度には以下の研究成果を得たので報告する。

1）リードスルー現象を定量化するために我々が開発したダブルレポーター遺伝子を導入したトランスジェニックマウスを用いてゲンタマイシンの経皮的投与により、骨格筋組織にリードスルーが惹起されることを示した。

2）上記マウスを用いてゲンタマイシン類縁抗菌物質のリードスルー活性を検討したところ、ゲンタマイシンと同等の活性を示す物質が存在した。

3) ネガマイシンの分子構造と類似した立体構造を持つ物質のin silico探索を行って得た候補物質を実際に入手し、上記トランスジェニックマウスに投与したところ、リードスルー活性を示す新規薬物候補物質を得ることが出来た。

本研究実施にあたり、平成１７年度厚生労働省科学研究費「こころの健康科学研究事業」のご援助をいただいたことに深く感謝いたします。

平成18年4月7日　主任研究者　松田良一（東京大学大学院総合文化研究科）

交付額平成17年度　9,482千円　（直接研究費のみ）

様式A-1（5）

厚生労働科学研究費補助金研究報告書

平成18年4月7日

厚生労働大臣　川崎二郎　殿

〒153-8902　東京都目黒区駒場3-8-1

マツダ　リョウイチ
研究者　松田　良一

（所属機関　東京大学大学院 総合文化研究科）

平成17年度厚生労働科学研究費補助金（こころの健康科学研究事業）に係わる研究事業を完了したので次のとおり報告する。

研究課題名（課題番号）：ナンセンス変異型筋ジストロフィーのリードスルー薬物による治療法の確立（H16-こころ-027）

国庫補助金精算所要額　：金　9,482,000円也（うち間接経費　0円）

1．厚生労働科学研究費補助金研究報告書表紙　（別添１のとおり）
2．厚生労働科学研究費補助金研究報告書目次　（別添２のとおり）
3．厚生労働科学研究費補助金総括研究報告書　（別添３のとおり）
4．厚生労働科学研究費補助金分担研究報告書　（別添４のとおり）
5．研究成果の刊行に関する一覧表　（別添５のとおり）
6．研究成果による特許権等の知的財産権の出願・登録状況
（総括研究報告書、分担研究報告書の中に、書式に従って記入すること）
7．健康危険情報

・研究の結果、得られた成果の中で健康危険情報（国民の生命、健康に重大な影響を及ぼす情報として厚生労働省に報告すべきものがある場合や、研究過程において健康危険情報を把握した場合には、国民の生命、健康に重大な影響を及ぼすと考えられる内容と理由を簡潔に記入するとともに、その情報源（研究成果、研究者名、学会発表名、雑誌等の詳細）について記述すること。

・既に厚生労働省に通報した健康危険情報であっても、本研究報告書の提出の時点において健康危険情報に該当すると判断されるものについては記述すること。

・分担研究者、研究協力者の把握した情報・意見等についても主任研究者がとりまとめ、一括して総括研究報告書に記入すること。

・なお、交付基準額等決定通知の添付文書において、健康危険情報を把握した際には、一定の書式で速やかに厚生労働省健康危機管理官まで通報していただくよう協力をお願いしているので、本件とともに留意すること。

厚生労働科学研究費補助金（こころの健康科学研究事業）
総括研究報告書

ナンセンス変異型筋ジストロフィーのリードスルー薬物による治療法の確立

主任研究者　松田良一　東京大学大学院総合文化研究科 助教授

研究要旨

点変異により生じた未熟終止コドン（Premature Termination Codon；PTC）を薬物により読み越え【リードスルー】させ，野生型正常タンパク質を作らせることができれば，単一遺伝性疾患の3割を占めるナンセンス変異型筋ジストロフィーの化学治療が可能になる。本研究は，独自のリードスルー活性解析系として，3種（TAA，TAG，TGA）のPTCをそれぞれ挿入したβ-ガラクトシダーゼとルシフェラーゼのデュアルレポーター遺伝子を組み込んだ3種のトランスジェニック（Tg）マウス系統を作成し，これらのTgマウスを用いてリードスルー薬物の投与経路や投与量の最適化を行い，リードスルー薬物のナンセンス変異型筋ジストロフィーに対する治療効果を検証することを目的としている。今年度は，リードスルー活性検出系となるデュアルレポーターTgマウスを用いて，in silico検索により選定された，ネガマイシンの立体配位形成に適合する類似物質群のリードスルー活性を検討したところ，現在までに新規リードスルー惹起物質を4種見出した。また，アミノグリコシド系抗菌性物質製剤からゲンタマイシンC1aのジヒドロ体であるシソマイシンや，ゲンタマイシンC2bであるミクロノマイシンのリードスルー活性を確認した。シソマイシンは聴覚・腎毒性が低いことから，その意義は大きいと考えられる。さらに，抗菌性物質の皮膚外用剤によるリードスルー活性の評価を行ったところ，経皮投与群でのルシフェラーゼ活性の有意な蓄積を検出し，等用量のゲンタマイシンの経皮／皮下投与の比較では，経皮投与による高いリードスルー活性を確認した。また皮膚外用剤は油脂性基剤（軟膏）よりも乳剤性基剤（クリーム）のほうが薬物透過性が高く，投与に適していることを確認した。皮膚を介した投与法は，局所的に適用することが可能で，消化器系副作用が少なく，持続性があり，投与による負担を軽減できるなど有用性が高いと考えられるため，経皮治療システムでナンセンス変異型筋ジストロフィーを克服する可能性を提示した。

分担研究者

池田大四郎（財団法人微生物化学研究会
微生物化学研究センター
副センター長）

A. 研究目的

点変異により生じた未熟終止コドン（Premature Termination Codon；PTC）を薬物により読み越え【リードスルー】させ，野生型正常タンパク質を作らせることができれば，単一遺伝性疾患の3割を占めるナンセンス変異型筋ジストロフィーの化学治療が可能になる。本研究は，独自のリードスルー活性解析系として，3種（TAA，TAG，TGA）のPTCをそれぞれ挿入したβ-ガラクトシダーゼとルシフェラーゼのデュアルレポーター遺伝子を組み込んだ3種のトランスジェニック（Tg）マウス系統を作成し，これらのTgマウスを用いてリードスルー薬物の投与経路や投与量の最適化を行い，リードスルー

薬物のナンセンス変異型筋ジストロフィーに対する治療効果を検証することを目的としている。

B. 研究方法

Tgマウスの確立

β-ガラクトシダーゼとルシフェラーゼ遺伝子を連結し，その繋ぎ目に3種類の終止コドンを挿入した3種類のコンストラクト（mdxマウスのエクソン23のPTC前後12mer周辺配列を含む27mer）を含む，サイトメガロウイルスエンハンサー／ニワトリβーアクチンハイブリッドプロモーターを有する発現ベクター（pCAGGS）を生殖細胞系列に組み込んだTgマウス系統を作出した。PTC部位にはOchre, Amber, Opal（TAA, TAG, TGA）をそれぞれ挿入した。

リードスルー惹起薬物の探索

ゲンタマイシン関連アミノグリコシド系抗菌性物質製剤及びin silico三次元データ解析により105万種以上の化合物から選定された，ネガマイシンの立体配位形成に適合する類似物質から選定した化合物をTgマウスに一週間連日皮下投与した後，大腿部骨格筋組織抽出液のルシフェラーゼ活性とβ-ガラクトシダーゼ活性をルミノメータで定量し，リードスルー活性をルシフェラーゼ／β-ガラクトシダーゼとして算出した。

経皮投与によるリードスルー惹起

ゲンタマイシン皮膚外用剤（1mg力価/1g）を，背・腰・腿部を除毛したTgマウスに一週間連日単純塗擦し，投与箇所直下の背筋・大臀筋・大腿筋の組織抽出液のβ-ガラクトシダーゼ活性とルシフェラーゼ活性を測定し，リードスルー活性を算出した。

（倫理面への配慮）

平成17年6月第162国会において改正された「動物の愛護及び管理に関する法律（法律第68号）」と，実験動物の飼養及び保管等に関する基準（総理府告示第6号）」に基づいて動物実験を実施した。具体的に，麻酔使用による苦痛の除去・軽減，培養細胞を用いた代替法の活用を徹底し，適切に利用することに配慮した。Tgマウスを用いたリードスルー活性の検出，mdxマウスを用いたジストロフィン発現の検出等については，東京大学大学院と財団法人微生物化学研究会の各動物実験委員会と組み替えDNA実験委員会の審査・承認を得て，動物実験の手引きに策定されている指針に従い，計画的な条件選定の下，実験を行った。倫理的・法的・社会的問題に関わる全ての指針を遵守することで，研究が適正に推進されるよう配慮した。

C. 研究結果

Tgマウスの確立

Ochre, Amber, Opal（TAA, TAG, TGA）のPTCをそれぞれ挿入したデュアルレポーターTgマウス3系統を確立した。骨格筋，心筋，脳での強いβ-ガラクトシダーゼの発現が確認された。

リードスルー惹起薬物の探索

リードスルー活性検出系となるデュアルレポーターTgマウスを用いて，in silico検索により選定された，ネガマイシンの立体配位形成に適合する類似物質群のリードスルー活性を検討したところ，現在までに新規リードスルー惹起物質を4種見出した。また，アミノグリコシド系抗菌性物質製剤からゲンタマイシンC1aのジヒドロ体であるシソマイシンや，ゲンタマイシンC2bであるミクロノマイシンのリードスルー活性を確認した。

経皮投与によるリードスルー惹起

抗菌性物質の皮膚外用剤によるリードスルー活性の評価を行ったところ，経皮投与群でのルシフェ

ラーゼ活性の有意な蓄積を検出し，等用量のゲンタマイシンの経皮／皮下投与の比較では，経皮投与による高いリードスルー活性を確認した。

D. 考察

Tgマウスの確立

3種のTgマウスについては，脳，肺，肝臓，膵臓，小腸，脾臓，腎臓，心筋，骨格筋（大腿筋，前頸骨筋，横隔膜）の各臓器の凍結切片のX-gal染色と組織抽出液からのβ-ガラクトシダーゼ発現を指標に，更なる発現能力の強化や感受性範囲の拡大を図るため交配を重ねている。作成した3種のTgマウス系統は，薬物および変異原解析系として汎用性が高いモデル動物となるため，更なるレポーター遺伝子発現能力の強化や感受性範囲の拡大を図り交配を重ねた上で，使用法特許を取得する。これらの知的財産は今後の創薬研究に貢献し，その技術開発に提供できうる強力なツールとなる。

これらTgマウスの感受性を高めた上で薬物投与の際に，ルシフェリンを静脈注射して発生する光子を高感度CCDで検出し，そのイメージ画像解析による非侵襲的なリードスルー活性の経時的測定系を確立することと，スクエア波パルスを用いた電気的導入法によるドラッグデリバリーの効率化を検討している。

リードスルー惹起薬物の探索

現在までに見出された4種のリードスルー惹起新規化合物は比較的低分子であることから，今後の開発に期待をもつことができ，有機化学的展開と質量分析を用いた構造活性相関から，薬効の増強，副作用の軽減，溶解性・安定性・吸収性の改善を計り，分子設計と合成展開により創出された新規物質について物質特許或いは使用法特許を取得する。また，リードスルー惹起物質としてのシソマイシンは聴覚・腎毒性が低いとされていることから，その意義は大きいと考えられる。

血清検体の薬物濃度測定により，候補薬物の吸収，分布，代謝，排泄，毒性について解析を行い，得られた薬物動態プロファイルから，投与経路・量・間隔等の最適化を検討すると共に，複数薬物の投与効果や，疾患に合わせた標的組織特異的かつ効率的なドラッグデリバリーシステムを検証する。

経皮投与によるリードスルー惹起

皮膚外用剤は油脂性基剤（軟膏）よりも乳剤性基剤（クリーム）のほうが薬物透過性が高く，投与に適していることを確認した。皮膚を介した投与法は，局所的に適用することが可能で，消化器系副作用が少なく，持続性があり，投与による負担を軽減できるなど有用性が高いと考えられる。現在製薬会社と共同で，吸収効率・持続性を考慮した製剤法の改良を検討している。

E. 結論

リードスルー活性を測定するためにデュアルレポーター遺伝子を持つTgマウスを作成した。これらを用いてゲンタマイシンやネガマイシンの類似物質のリードスルー活性を検討したところ，4種の新規リードスルー惹起物質を見出した。これらについては，更にその作用部位における量的および質的な経時的変化や濃度と薬効との関係，毒性等の検討が必要である。また，経皮治療システムでナンセンス変異型筋ジストロフィーを克服する可能性を提示した。

F. 健康危険情報

G. 研究発表

1. 論文発表

Nagata Y, Kobayashi H, Umeda M, Ohta N, Kawashima S, Zammit PS, and Matsuda R; Sphingomyelin Levels in the Plasma Membrane Correlate with the Activation State of Muscle Satellite Cells. J. Histochem. Cytochem. 54:375-384

Yamane A, Akutsu S, Diekwisch TG, and Matsuda R; Satellite cells and utrophin are not directly correlated with the degree of skeletal muscle damage in mdx mice. Am. J. Physiol. Cell Physiol., 289:C42-48, (2005)

山内潤一郎，松田良一，H.L.Sweeney;遺伝子治療のアスレティックパーフォーマンスへの応用，そして悪用 2 Training Journal 307:66-71, (2005)

山内潤一郎，松田良一，H.L. Sweeney;遺伝子治療のアスレティックパーフォーマンスへの応用，そして悪用 1 Training Journal 306:82-86, (2005)

2. 学会発表

Watanabe K, Fujiyama T, Miyazaki K, Shiozuka M, and Matsuda R, Fabrication of Growth Factor Array Using a Color Ink Jet Printer. 2nd International Bioprinting, Biopatterning Workshop (2005)

Shiozuka M, Shimada K, and Matsuda R, Establishment of dual reporter transgenic mice for read-through assay. FASEB Summer Research Conference 4th "Muscle satellite & stem cell" (2005)

Shiozuka M, Shimada K, and Matsuda R, Development of dual-reporter transgenic mice for readthrough assay. The American Society for Cell Biology 45th Annual Meeting (2005)

Kikkawa N, Shiozuka M, Kogure T, and Matsuda R, Visualization of ectopic calcification in mdx mouse skeletal muscle 2 The American Society for Cell Biology 45th Annual Meeting (2005)

長田洋輔，Zammit P，Partridge T，松田良一，スフィンゴシン-1-リン酸による筋衛星細胞の活性化 日本動物学会第76回大会 (2005)

吉川奈美子，松田良一，mdxマウス骨格筋の遺書的石灰化 (2) 日本動物学会第76回大会 (2005)

塩塚政孝，嶋田健一，松田良一，リードスルー活性検出系としてのデュアルレポータートランスジェニックマウスの開発 日本動物学会第76回大会 (2005)

H. 知的財産の出願・登録状況

1. 特許取得
2. 実用新案登録
3. その他

厚生労働科学研究費補助金（こころの健康科学研究事業）
分担研究報告書

リードスルー薬剤のサンプル提供

主任研究者　池田大四郎　財団法人微生物化学研究会 微生物化学研究センター
副センター長

研究要旨
アミノグリコシド抗生物質の提供とそれらのリードスルー活性から，構造活性相関を検討した。

A. 研究目的

アミノグリコシド抗生物質のリードスルー活性についてそれらの構造活性相関を検討する

アミノグリコシド抗生物質（ＡＧ）は、バクテリアのrRNAに作用し、そのタンパク質合成を阻害することにより、殺菌的抗菌剤として広く臨床で使用されている。一方、近年真核細胞においてＡＧが終止コドンの読み越え活性を有することが報告されている。当研究センターは、過去にジベカシン、アルベカシンなどのアミノグリコシド抗生物質を創製、開発した経緯から、本プロジェクトにおいて、新たなリードスルー活性を有する薬剤を見いだすために、各種ＡＧを提供しそれらの構造活性相関を検討した。

C. 研究結果

各種ＡＧのうち、ゲンタミシン群とネオマイシン群にリードスルー活性があることを見出した。

G. 研究発表

1. 論文発表

Momose I, Umezawa Y, Hirosawa S, Iijima M, Iinuma H, and Ikeda D. Synthesis and activity of tyropeptin A derivatives as potent and selective inhibitors of mammalian 20S proteasome. Biosci. Biotechnol. Biochem., 69, 1733-1742 (2005)

2. Yoshimoto Y, Kawada M, Kumagai H, Someno T, Inoue H, Kawamura N, Isshiki K and Ikeda D. New naphthoquinones, f13102A and B, from a fungas strain F13102. J. Antibiotics, 58, 590-593 (2005)

Takamoto K, Kawada M, and Ikeda D. Prevention of neomycin-induced nephrotoxic event in pig proximal tubular epithelial cell line by apolipoprotein E3. J. Antibiotics, 58, 353-355. (2005)

Momose I, Umezawa Y, Hirosawa S, Iinuma H, and Ikeda D. Structure-based design of derivatives of tyropeptin A as the potent and selective inhibitors of mammalian 20S proteasome. Bioorg. Med. Chem. Lett., 15, 1867-1871. (2005)

Takamoto K, Kawada M, Ikeda D, and Yoshida M. Apolipoprotein E3 (apoE3) safeguards pig proximal tubular LLC-PK1 cells against reduction in SGLT1 activity induced by gentamicin C. Biochim. Biophys. Acta-Gen. Sub, 1722, 247-253. (2005)

Kumagai H, Wakazono K, Agata N, Isshiki K, Ishizuka M, and Ikeda D. Effect of cytogenin, a novel immunomodulator, on streptozotocin-induced diabetes in mice. J. Antibiotics, 58, 202-205. (2005)

Someno T, Kunimoto S, Nakamura H, Naganawa H, and Ikeda D. Absolute configuration of kigamicins A, C and D. J. Antibiotics, 58, 56-60. (2005)

Yoshimoto Y, Kawada M, Ikeda D, and Ishizuka M. Involvement of doxorubicin-induced Fas expression in the antitumor effect of doxorubicin on Lewis lung carcinoma in vivo. Int. Immunopharmacol., 5, 281-288. (2005)

研究成果の刊行に関する一覧表

雑誌

Nagata Y, Kobayashi H, Umeda M, Ohta N, Kawashima S, Zammit PS, and Matsuda R; Sphingomyelin Levels in the Plasma Membrane Correlate with the Activation State of Muscle Satellite Cells. J. Histochem. Cytochem. 54:375-384

Yamane A, Akutsu S, Diekwisch TG, and Matsuda R; Satellite cells and utrophin are not directly correlated with the degree of skeletal muscle damage in mdx mice. Am. J. Physiol. Cell Physiol., 289:C42-48, (2005)

山内潤一郎, 松田良一, H.L.Sweeney;遺伝子治療のアスレティックパーフォーマンスへの応用, そして悪用 2 Training Journal 307:66-71, (2005)

山内潤一郎, 松田良一, H.L. Sweeney;遺伝子治療のアスレティックパーフォーマンスへの応用, そして悪用 1 Training Journal 306:82-86, (2005)

Momose I, Umezawa Y, Hirosawa S, Iijima M, Iinuma H, and Ikeda D. Synthesis and activity of tyropeptin A derivatives as potent and selective inhibitors of mammalian 20S proteasome. Biosci. Biotechnol. Biochem., 69, 1733-1742 (2005)

Yoshimoto Y, Kawada M, Kumagai H, Someno T, Inoue H, Kawamura N, Isshiki K and Ikeda D. New naphthoquinones, f13102A and B, from a fungas strain F13102. J. Antibiotics, 58, 590-593 (2005)

Takamoto K, Kawada M, and Ikeda D. Prevention of neomycin-induced nephrotoxic event in pig proximal tubular epithelial cell line by apolipoprotein E3. J. Antibiotics, 58, 353-355. (2005)

Momose I, Umezawa Y, Hirosawa S, Iinuma H, and Ikeda D. Structure-based design of derivatives of tyropeptin A as the potent and selective inhibitors of mammalian 20S proteasome. Bioorg. Med. Chem. Lett., 15, 1867-1871. (2005)

Takamoto K, Kawada M, Ikeda D, and Yoshida M. Apolipoprotein E3 (apoE3) safeguards pig proximal tubular LLC-PK1 cells against reduction in SGLT1 activity induced by gentamicin C. Biochim. Biophys. Acta-Gen. Sub, 1722, 247-253. (2005)

Kumagai H, Wakazono K, Agata N, Isshiki K, Ishizuka M, and Ikeda D. Effect of cytogenin, a novel immunomodulator, on streptozotocin-induced diabetes in mice. J. Antibiotics, 58, 202-205. (2005)

Someno T, Kunimoto S, Nakamura H, Naganawa H, and Ikeda D. Absolute configuration of kigamicins A, C and D. J. Antibiotics, 58, 56-60. (2005)

Yoshimoto Y, Kawada M, Ikeda D, and Ishizuka M. Involvement of doxorubicin-induced Fas expression in the antitumor effect of doxorubicin on Lewis lung carcinoma in vivo. Int. Immunopharmacol., 5, 281-288. (2005)

Am J Physiol Cell Physiol 289: C42–C48, 2005.
First published February 9, 2005; doi:10.1152/ajpcell.00577.2004.

Satellite cells and utrophin are not directly correlated with the degree of skeletal muscle damage in *mdx* mice

Akira Yamane,[1] Satonari Akutsu,[2] Thomas G. H. Diekwisch,[3] and Ryoichi Matsuda[4]

[1]*Department of Pharmacology and* [2]*High Technology Research Center, Tsurumi University School of Dental Medicine, Yokohama, Japan;* [3]*Brodie Laboratory for Craniofacial Genetics, Department of Orthodontics, University of Illinois College of Dentistry, Chicago, Illinois; and* [4]*Department of Biology, The University of Tokyo, Tokyo, Japan*

Submitted 29 November 2004; accepted in final form 3 February 2005

Yamane, Akira, Satonari Akutsu, Thomas G. H. Diekwisch, and Ryoichi Matsuda. Satellite cells and utrophin are not directly correlated with the degree of skeletal muscle damage in *mdx* mice. *Am J Physiol Cell Physiol* 289: C42–C48, 2005. First published February 9, 2005; doi:10.1152/ajpcell.00577.2004.—To determine whether muscle satellite cells and utrophin are correlated with the degree of damage in *mdx* skeletal muscles, we measured the area of the degenerative region as an indicator of myofiber degeneration in the masseter, gastrocnemius, soleus, and diaphragm muscles of *mdx* mice. Furthermore, we analyzed the expression levels of the paired box homeotic gene 7 (*pax7*), m-cadherin (the makers of muscle satellite cells), and utrophin mRNA. We also investigated the immunolocalization of m-cadherin and utrophin proteins in the muscles of normal C57BL/10J (B10) and *mdx* mice. The expression level of *pax7* mRNA and the percentage of m-cadherin-positive cells among the total number of cell nuclei in the muscle tissues in all four muscles studied were greater in the *mdx* mice than in the B10 mice. However, there was no significant correlation between muscle damage and expression level for *pax7* mRNA ($R = -0.140$), nor was there a correlation between muscle damage and the percentage of satellite cells among the total number of cell nuclei ($R = -0.411$) in the *mdx* mice. The expression level of utrophin mRNA and the intensity of immunostaining for utrophin in all four muscles studied were greater in the *mdx* mice than in the B10 mice. However, there also was not a significant correlation between muscle damage and expression level of utrophin mRNA ($R = 0.231$) in the *mdx* mice, although upregulated utrophin was incorporated into the sarcolemma. These results suggest that satellite cells and utrophin are not directly correlated with the degree of skeletal muscle damage in *mdx* mice.

dystrophy; *pax7*; m-cadherin; dystrophin-related proteins

THE X CHROMOSOME-LINKED MUSCULAR dystrophic *mdx* mouse lacks the sarcolemmal protein dystrophin and represents a genetic homolog of human Duchenne muscular dystrophy. Dystrophin is a 427-kDa cytoskeletal protein that is expressed in the sarcolemma (the membrane structure of the myofiber) and contributes to the stability of the sarcolemma. Lack of dystrophin causes myofiber degeneration caused by membrane damage, Ca^{2+} overuptake by muscle cells, muscle overcontraction, and activation of intracellular proteinase (2, 8). The damage to myofibers varies among the muscles of the *mdx* mouse; the *mdx* diaphragm muscle is damaged more severely by dystrophy than are the other muscles (10, 27), whereas craniofacial muscles such as the masseter and extraocular muscles are less damaged (16, 20). However, the mechanism underlying differences in the degree of myofiber damage among *mdx* skeletal muscles is unclear.

Muscle satellite cells are mononucleated, quiescent stem cells that reside between the sarcolemma and the basal lamina of adult myofibers (4, 13). In response to stimuli such as mechanical loading, unloading, denervation, and injury, the satellite cells are activated to proliferate, differentiate into myoblasts, and fuse to preexisting myofibers. This activation is thought to induce adaptive changes of skeletal muscle such as hypertrophy, the alteration of fiber type, and regeneration (1, 4, 13, 23). These observations suggest that the activity and pool size of satellite cells are correlated with the degree of damage in *mdx* skeletal muscles.

Utrophin is a paralog of dystrophin and can functionally replace dystrophin (2, 7, 30). In normal adult myofibers, the expression of utrophin is confined to the neuromuscular and myotendinous junctions, whereas in *mdx* myofibers, utrophin is expressed throughout the sarcolemma instead of dystrophin, and the total amount of utrophin is markedly elevated compared with that in normal myofibers (2, 33). Moreover, transgenic *mdx* mice displaying fairly high amounts of utrophin show a complete correction of the dystrophic status (30). On the other hand, *mdx* mice in which the utrophin gene is inactivated present a catastrophic aggravation of myopathy, leading to early death (6). The situation in *mdx* muscles, however, lies between these latter two extremes. It seems important to know whether the spontaneous level of utrophin expression is negatively correlated with the degree of damage in *mdx* skeletal muscles.

In the present study, to determine whether muscle satellite cells and the expression of utrophin are correlated with the degree of damage in *mdx* skeletal muscles, we measured the area of the degenerative region relative to the total muscle area, an indicator of myofiber degeneration, in the masseter, gastrocnemius, soleus, and diaphragm muscles of the *mdx* mouse. Furthermore, we analyzed the mRNA expression levels of the paired box homeotic gene 7 (*pax7*), m-cadherin (maker of muscle satellite cells), and utrophin and investigated the immunolocalization of m-cadherin and utrophin in the muscles of both normal and *mdx* mice.

MATERIALS AND METHODS

Experimental animals. Dystrophic *mdx* and control C57BL/10J (B10) mice, obtained from the Central Animal Research Laboratory (Kanagawa, Japan), were used throughout the present study. All mice

Address for reprint requests and other correspondence: A. Yamane, Dept. of Pharmacology, Tsurumi Univ. School of Dental Medicine, 2-1-3 Tsurumi, Tsurumi-ku, Yokohama 230-8501, Japan (e-mail: yamane-a@tsurumi-u.ac.jp).

The costs of publication of this article were defrayed in part by the payment of page charges. The article must therefore be hereby marked "*advertisement*" in accordance with 18 U.S.C. Section 1734 solely to indicate this fact.

were maintained on a 12:12-h light-dark cycle, fed a pellet diet (CE-2; Clea Japan, Tokyo, Japan), and allowed access to tap water ad libitum. All experimental protocols concerning animal handling were reviewed and approved by the Institutional Animal Care Committee of the Tsurumi University School of Dental Medicine.

Histological analysis of degenerative area. Six *mdx* and six control B10 mice, aged 6 wk, were killed by cervical dislocation under ether anesthesia. The body weights of the *mdx* and B10 mice were 17.2 ± 1.9 g and 18.9 ± 1.5 g (mean ± SD), respectively. Whole portions of the left masseter, gastrocnemius, soleus, and diaphragm muscles were removed and fixed in Bouin's fixative for 1 h at 4°C. After being washed in phosphate-buffered saline (PBS), the sections were immersed in a graduated series of sucrose solutions (~20–40% wt/vol) in PBS at 4°C, embedded in Tissue-Tek OCT compound (Miles Laboratories, Elkhart, IN), and frozen. Middle portions of the muscles were cut at 10-μm thickness using a cryostat and air dried for 1 h at room temperature. The sections were stained with hematoxylin and eosin and observed under a light microscope. The total and degenerative areas of the muscle sections were measured using an image analyzer (Luzex 3U; Nikon, Tokyo, Japan). The degenerative area was normalized to the total area and expressed as a percentage of the total area of the muscles.

Immunohistochemistry for m-cadherin and utrophin. To detect the satellite cells in the *mdx* and B10 muscles, the cryosections of the muscles were immunostained for a goat antibody against m-cadherin (Santa Cruz Biotechnology, Santa Cruz, CA) as described previously (31). The number of m-cadherin-positive cells in the periphery of myofibers and in the degenerative area was counted as satellite cells in a total of 10 rectangular areas of 140 × 130 μm² on several sections obtained from each mouse (21). The 10 rectangular areas, which did not overlap and were uniformly distributed on the sectional area of muscles, were selected throughout the several sections and composed ~5–20% of the total sectional area of the B10 and *mdx* muscles. The number of total cell nuclei in muscle tissues was also counted, and the percentage of m-cadherin-positive cells to the total number of cell nuclei in the muscle tissues was calculated. The percentage values in the 10 rectangular areas were averaged to obtain the mean value for each mouse. This mean value was further averaged to obtain the mean values for six *mdx* and six B10 mice. To analyze the change in the expression of utrophin, immunostaining for utrophin was performed using a goat antibody against utrophin (Santa Cruz Biotechnology). For control staining, the primary antibody was replaced with PBS or normal goat IgG.

RNA extraction, reverse transcription, and competitive polymerase chain reaction amplification. Six *mdx* and six B10 mice, aged 6 wk, were killed by cervical dislocation while they were under ether anesthesia. The body weights of the *mdx* and B10 mice were 19.8 ± 0.8 g and 24.3 ± 0.5 g (means ± SD), respectively. Whole portions of the left masseter, gastrocnemius, soleus, and diaphragm muscles were removed, immediately frozen, and stored at −80°C until use.

Total RNA extraction, reverse transcription, and competitive polymerase chain reaction (PCR) amplification were performed as previ-

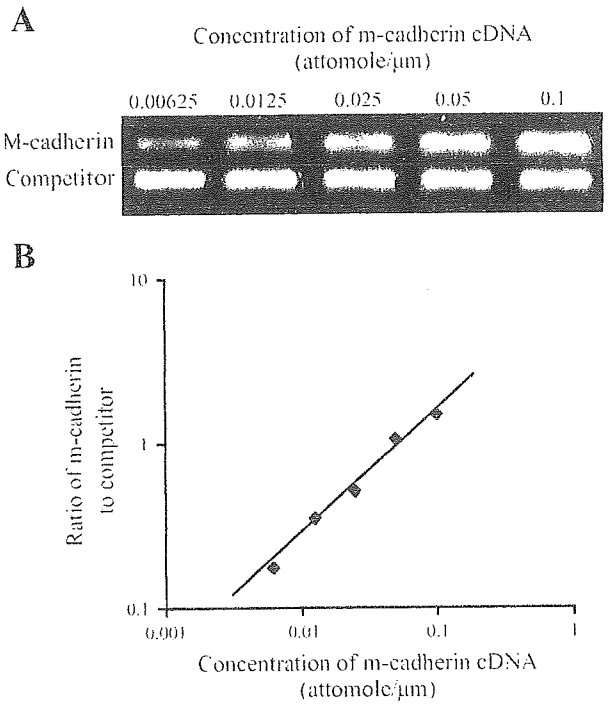

Fig. 1. *A*: electrophoretic gel pattern of m-cadherin and its competitor after competitive polymerase chain reaction (PCR) to examine the relationship between the amount of PCR products and the concentration of m-cadherin cDNA. Target gene is shown in *top* band, while competitor is shown in *bottom* band. *B*: regression line for the m-cadherin generated from the result of image analysis of the electrophoretic bands in *A*. The formula used to create the regression line is $y = 0.772x + 0.978$, where y is the logarithmic value of the ratio of the fluorescence intensity in the m-cadherin band to that in its competitor band, and x is the logarithmic value of the concentration of the m-cadherin cDNA.

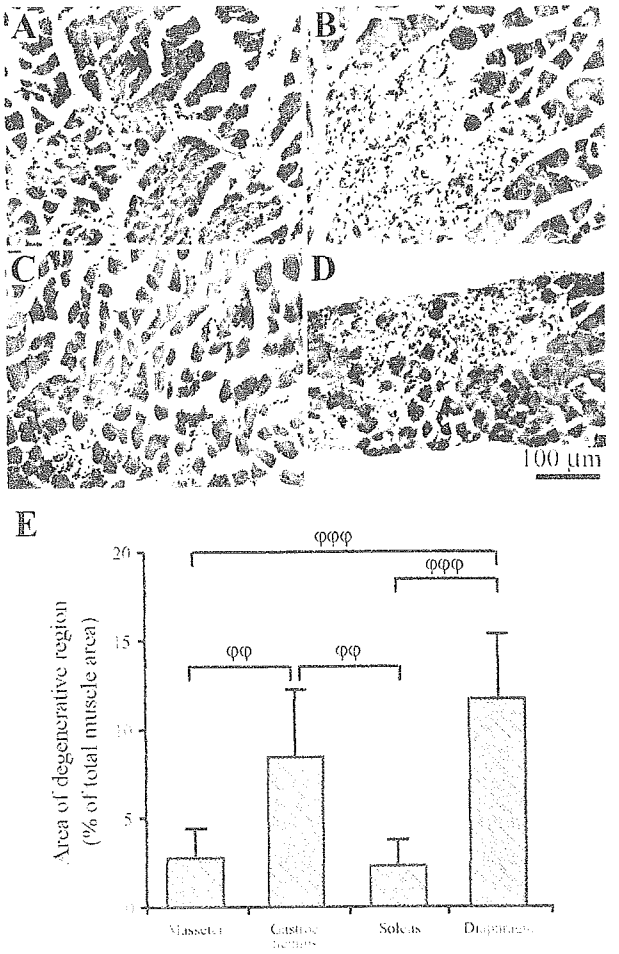

Fig. 2. *A–D*: hematoxylin and eosin-stained images of the masseter (*A*), gastrocnemius (*B*), soleus (*C*), and diaphragm (*D*) muscles of *mdx* mice. *E*: area of the degenerative region is shown relative to the total muscle area of the *mdx* mice. Each column and vertical bar represent the mean ± SD of six *mdx* mice. The *y*-axis is expressed as a percentage of the total sectional area of the muscles set at 100. $\phi\phi P < 0.01$ and $\phi\phi\phi P < 0.001$, significant differences among *mdx* muscles.

ously described (34, 36). Briefly, total RNA extraction was performed according to the manufacturer's specifications (rapid total RNA isolation kit; 5 Prime-3 Prime, Boulder, CO). The RNA was treated with 2 U of ribonuclease-free deoxyribonuclease I (Life Technologies, Gaithersburg, MD) and was then reverse transcribed with 200 U of reverse transcriptase (SuperScript II; Life Technologies).

In the conventional PCR technique, a small difference in the starting amount of target DNA can result in a large change in the yield of the final product, owing to the exponential nature of the PCR reaction. A plateau effect after many cycles can lead to an inaccurate estimation of final product yield. Furthermore, because the PCR amplification depends on the reaction efficiency, small changes in efficiency can lead to major differences in the final product yield. To overcome these problems, the competitor (an internal standard), which has the same primer sequences as those of the target DNA at the 5′ and 3′ ends, was amplified simultaneously with the target (11, 25, 34, 36). Competitors for the competitive PCR amplification were constructed according to the manufacturer's instructions (Competitive DNA Construction Kit; Takara, Shiga, Japan). The sequences of primers for *pax7*, m-cadherin, and utrophin were as follows: *pax7*, FW, 5′-CCACAGCTTCTCCAGCTACTCTG-3′ and BW, 5′-CACTCGGGTTGCTAAGGATGCTC-3′ (29); m-cadherin, FW, 5′-ATGTGCCACAGCCACATCG-3′ and BW, 5′-YCCATACATGCTCGCCAGC-3′ (14); utrophin, FW, 5′-AAACTCCTATCACGCTCATCA-3′ and BW, 5′-CTCATCCTCCACGCTTCCT-3′ (9). Those for S16 were identical to those used in a previous report (18). The amplification products were isolated by performing electrophoresis with an agarose gel containing ethidium bromide. The fluorescence intensities of the bands of the target genes (Fig. 1*A*, *top bands*) and their respective competitors (Fig. 1*A*, *bottom bands*) were measured using an image analyzer (Molecular Imager FX; Bio-Rad, Hercules, CA). We then calculated the ratios of the fluorescence intensities of the target gene bands to those of their respective competitors. The logarithmic value of the fluorescence intensity ratio was used to calculate the amount of endogenous target mRNA on the basis of the line formula derived from a standard curve for each target gene. The standard curve was generated as described previously (18, 35). Figure 1*B* shows the standard curve for m-cadherin calculated using the image analysis data of electrophoretic bands shown in Fig. 1*A*. The slope of the regression line was 0.772, and the correlation coefficient was 0.994, which was significantly different from zero ($P < 0.001$). The quantity of each target gene was normalized to the quantity of S16 (ribosomal protein). The resulting ratio value in each sample was expressed as a percentage of the mean value for the B10 masseter muscle. Because each percentage value relative to the mean value for the B10 masseter muscle (% of B10 masseter value) was an arbitrary unit, it was used in the scatterplots shown in Figs. 3–5, although the scatterplots contain no data regarding the B10 muscles.

Statistical analyses. The Tukey-Kramer method was used to compare multiple combinations of two muscles among the four *mdx* muscles. Student's *t*-test was used to compare single combinations of the same types of muscles between the B10 and *mdx* mice. Regression analysis was used to examine the correlations in the *mdx* mice between the degenerative areas of the skeletal muscles and the expression levels for *pax7* or utrophin mRNA and between the degenerative areas of the skeletal muscles and the percentages of m-cadherin-positive cells to the total number of cell nuclei in the muscle tissues. Differences were considered significant at $P < 0.05$.

RESULTS

To detect the degenerative area of the *mdx* muscle, cryosections from the middle portions of the muscles were stained with hematoxylin and eosin (Fig. 2, *A–D*). In the *mdx* gastrocnemius and diaphragm muscles, histopathological changes such as myofiber degeneration (Fig. 2, *B* and *D*) were observed. By contrast, none of the muscles of the control B10 mice showed such histopathological changes (data not shown). Figure 2*E* shows the degenerative area relative to the total cross-sectional area of the *mdx* muscles. The degenerative areas of the diaphragm and gastrocnemius muscles were 11.7 ± 3.6% and 8.5 ± 3.7% of the total muscle areas, respectively. These areas were significantly greater than those of the masseter (2.8 ± 1.6%) and soleus muscles (2.4 ± 1.5%) ($P < 0.01$ to gastrocnemius and $P < 0.001$ to diaphragm).

To determine whether the activity and pool size of muscle satellite cells are correlated with the degree of damage in *mdx*

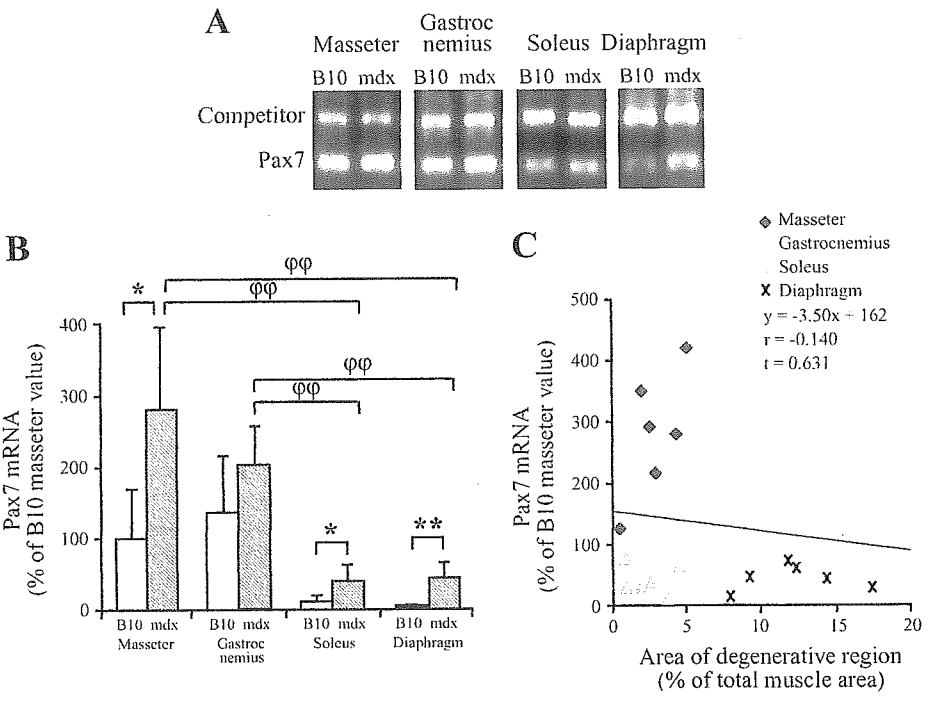

Fig. 3. *A*: typical example of gel electrophoretic pattern for paired box homeotic gene 7 (*pax7*)-competitive RT-PCR products of the masseter, gastrocnemius, soleus, and diaphragm muscles obtained from control C57BL/10J (B10) and *mdx* mice. The target gene is shown in the *bottom* bands, while the competitor is shown in the *top* band. *B*: mRNA expression levels for *pax7* in the masseter, gastrocnemius, soleus, and diaphragm muscles obtained from B10 and *mdx* mice. Each column and vertical bar represent the mean ± SD of six B10 or *mdx* mice. The *y*-axis is expressed as a percentage of the mean value of the B10 masseter muscle set at 100. $*P < 0.05$ and $**P < 0.01$, significant differences between B10 and *mdx* mice. $\phi\phi P < 0.01$, significant difference among *mdx* muscles. *C*: scatterplot and regression line between degenerative areas of skeletal muscles and expression levels of *pax7* in *mdx* mice.

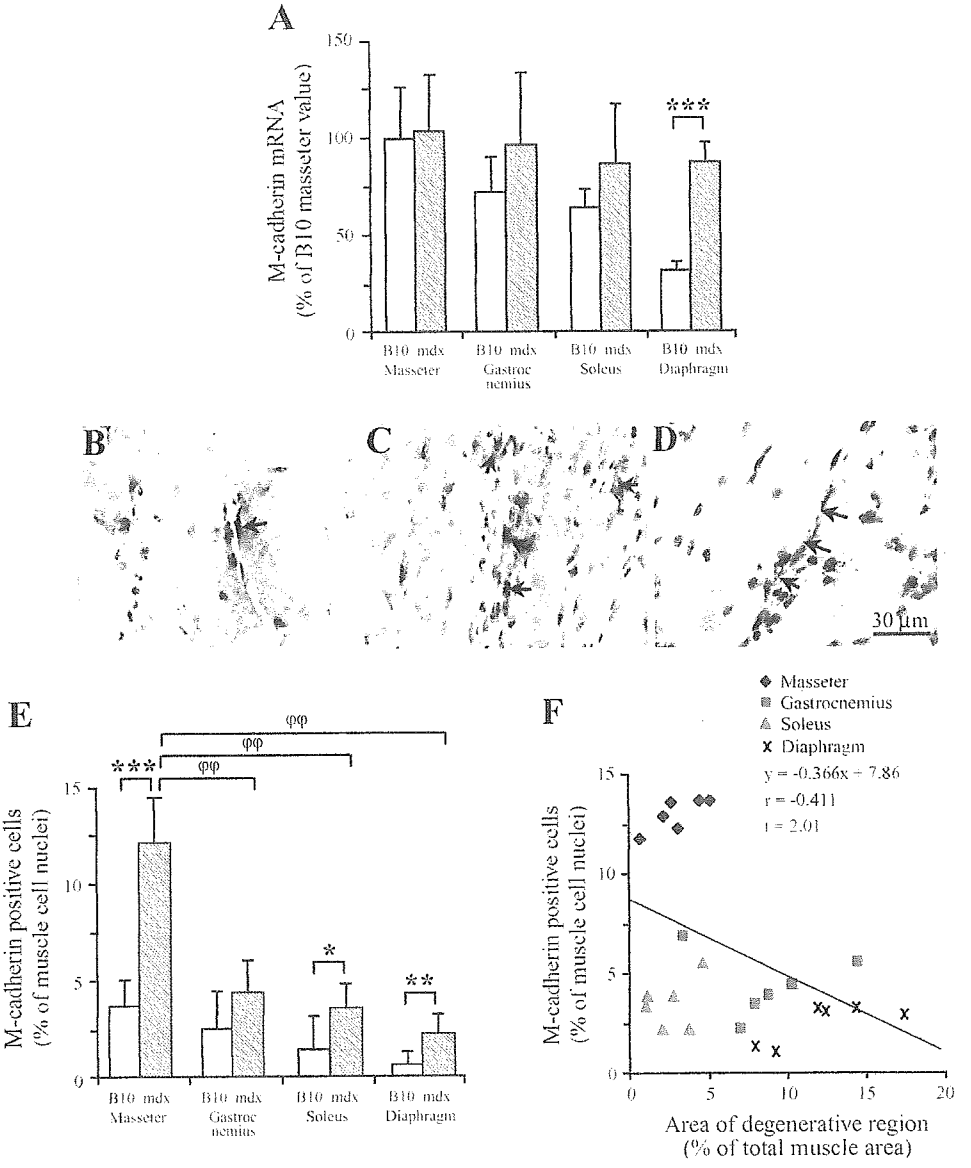

Fig. 4. *A*: mRNA expression levels for m-cadherin in the masseter, gastrocnemius, soleus, and diaphragm muscles obtained from B10 and *mdx* mice. Each column and vertical bar represent the mean ± SD of six B10 or *mdx* mice. The *y*-axis is expressed as a percentage of the mean value of the B10 masseter muscle set at 100. *B–D*: immunostaining images for m-cadherin in the *mdx* masseter muscle tissues. Arrows in *B* and *C* indicate the satellite cells identified by immunostaining for m-cadherin. Arrows in *D* indicate the m-cadherin-positive cells in the areas interspaced among the myofibers. *E*: ratio of satellite cells to total number of cell nuclei in the masseter, gastrocnemius, soleus, and diaphragm muscles obtained from B10 and *mdx* mice. Each column and vertical bar represent the mean ± SD of six B10 or *mdx* mice. $*P < 0.05$, $**P < 0.01$, and $***P < 0.001$, significant differences between B10 and *mdx* muscles. $\phi\phi P < 0.01$, significant difference among *mdx* muscles. *F*: scatterplot and regression line between degenerative areas of skeletal muscles and ratio of satellite cells to total number of cell nuclei in muscle tissues in *mdx* mice.

skeletal muscles, we analyzed the expression of *pax7* (Fig. 3) and m-cadherin (Fig. 4), which are both markers for muscle satellite cells. Figure 3*A* shows a typical gel electrophoretic pattern of *pax7*-competitive PCR products for the masseter, gastrocnemius, soleus, and diaphragm muscles of the B10 mice. The fluorescence intensities of the *pax7* bands (*bottom* band) and of its respective competitor bands (*top* band) were measured using an image analyzer. Image analysis of the PCR bands indicated that in all muscles studied except the gastrocnemius muscle, the expression levels of *pax7* mRNA were significantly higher in the *mdx* mice than in the B10 mice ($P < 0.05$ and $P < 0.01$) (Fig. 3*B*). In the *mdx* mice, the expression level for *pax7* mRNA in the masseter muscle was more than sixfold the levels in the soleus and diaphragm muscles ($P < 0.01$) but not significantly different from that in the gastrocnemius muscle. Figure 3*C* shows a scatterplot and a regression line between the degenerative areas of the skeletal muscles and the expression levels of *pax7* in the *mdx* mice. The correlation coefficient was −0.140, which was not significantly different from zero.

In all muscles studied, the mean values of the expression levels for m-cadherin mRNA were higher in the *mdx* mice than in the B10 mice; only the 2.4-fold increase in the diaphragm muscle was statistically significant (Fig. 4*A*). In the *mdx* mice, no significant difference in the expression levels for m-cadherin mRNA was found among the muscles. Because m-cadherin is reportedly expressed in neural cells within muscle tissues (19), we also investigated the immunolocalization of m-cadherin. The number of m-cadherin-positive cells in the periphery of myofibers (arrow in Fig. 4*B*) and in the degenerative area (arrows in Fig. 4*C*) was counted as satellite cells. M-cadherin-positive cells in the areas interspaced among myofibers (arrows in Fig. 4*D*) were excluded. In all muscles studied except the gastrocnemius muscle, the ratio of satellite cells to the total number of cell nuclei in the muscle tissues was significantly higher in the *mdx* mice than in the B10 mice ($P <$

0.05 and $P < 0.001$) (Fig. 4*E*). In the *mdx* mice, the percentage of satellite cells to the total number of cell nuclei in the muscle tissues in the masseter muscle was ~2.7- to 5.4-fold those in the other three muscle types ($P < 0.01$). The correlation coefficient between the degenerative areas of the skeletal muscles and the percentage of m-cadherin-positive cells to the total number of cell nuclei in the muscle tissues in the *mdx* mice was −0.411, which was not significantly different from zero (Fig. 4*F*).

To investigate the relationship between utrophin expression and the degree of damage in the *mdx* skeletal muscles, we analyzed the expression levels of utrophin mRNA and the immunolocalization of utrophin (Fig. 5). In all muscles studied, the mean values of the expression levels for utrophin mRNA were higher in the *mdx* mice than in the B10 mice, and the 1.4- and 3.0-fold increases in the soleus and diaphragm muscles, respectively, were statistically significant ($P < 0.05$ and $P < 0.001$) (Fig. 5*A*). In the *mdx* mice, the expression level of utrophin mRNA in the diaphragm muscle was ~1.4- to 2.7-fold ($P < 0.05$ and $P < 0.01$) the levels in the other three muscles, and that in the gastrocnemius muscle was ~2-fold ($P < 0.01$) the levels in the masseter and soleus muscles. The correlation coefficient between the degenerative areas of the skeletal muscles and the expression levels for utrophin mRNA in the *mdx* mice was 0.231, which was not significantly different from zero (Fig. 5*B*). In the B10 mice, immunostaining for utrophin was sporadically found in the periphery of myofibers (black arrowheads in Fig. 5, *C* and *E*). In the *mdx* masseter muscle, the periphery (black arrowheads) and the whole sarcoplasm of regenerative myofibers with central nuclei were immunostained for utrophin (Fig. 5*D*). The periphery of normal masseter myofibers without central nuclei (white arrowheads) was slightly stained, but the sarcoplasm (arrows) was not stained (Fig. 5*D*). In the *mdx* diaphragm muscle, immunostaining for utrophin was observed in both the whole sarcoplasm and the periphery of normal and degenerative myofibers, and the immunostaining in the periphery (sarcolemma) of myofibers (black arrowheads) was more intense than that in the sarcoplasm (Fig. 5*F*). The immunostaining patterns for utrophin in the gastrocnemius and soleus muscles were similar to those in the masseter muscle (data not shown).

DISCUSSION

In the course of skeletal muscle regeneration, quiescent satellite cells are activated to proliferate, and after several rounds of proliferation, the majority of satellite cells differentiate and fuse to form new myofibers or to repair damaged myofibers. We analyzed the expression of *pax7* and m-cadherin as markers for satellite cells. On the basis of their

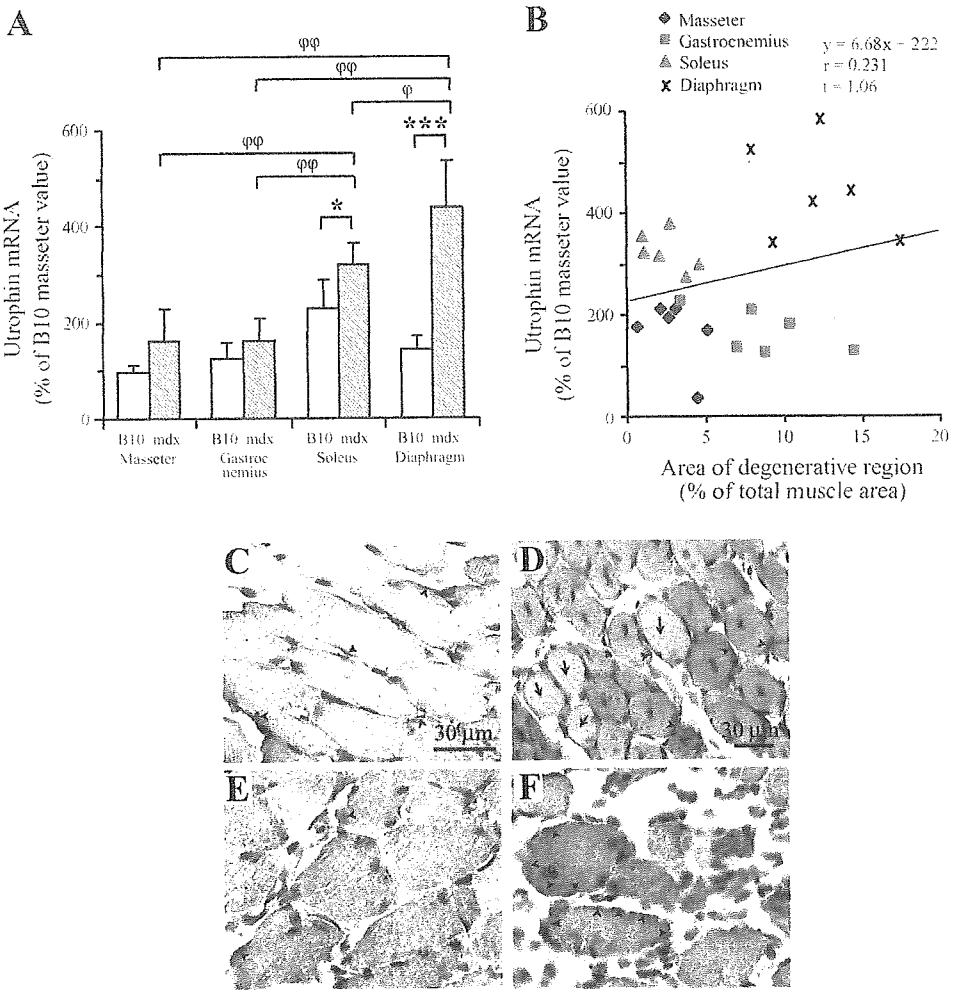

Fig. 5. *A*: mRNA expression levels for utrophin in the masseter, gastrocnemius, and diaphragm muscles obtained from B10 and *mdx* mice. Each column and vertical bar represent the mean ± SD of six B10 or *mdx* mice. The *y*-axis values are expressed as a ratio of the mean value of the B10 masseter muscle set at 100. $*P < 0.05$ and $***P < 0.001$, significant differences between B10 and *mdx* muscles. $\phi P < 0.05$ and $\phi\phi P < 0.01$, significant differences among *mdx* muscles. *B*: scatterplot and regression line between degenerative areas of skeletal muscles and expression levels of utrophin mRNA in *mdx* mice. *C–F*: immunostaining images for utrophin in the masseter (*C* and *D*) and diaphragm (*E* and *F*) muscle tissues of the B10 (*C* and *E*) and *mdx* (*D* and *F*) mice. Black and white arrowheads in *C–F* indicate immunostaining for utrophin in the periphery of the myofibers. Arrows in *D* indicate sarcoplasm of normal myofibers unstained for utrophin. Image shown in *E* was obtained at same original magnification as the one shown in *C*, and image shown in *F* was obtained at same original magnification as the one shown in *D*.

expression patterns and functions (4, 13, 15, 24), *pax7* and m-cadherin are considered markers for quiescent, activating, and proliferating satellite cells. In the present study, the expression level of *pax7* mRNA and the percentage of m-cadherin-positive cells to the total number of cell nuclei in the muscle tissues in all four muscles studied were greater in the *mdx* mice than in the B10 mice (Fig. 3*B* and 4*E*), suggesting that the activation and proliferation processes of muscle satellite cells occur more actively in *mdx* muscles than in B10 muscles. Reimann et al. (21) reported no significant difference in the percentage of m-cadherin-positive cells to the total number of cell nuclei in the soleus muscle between B10 and *mdx* mice, which appears to be inconsistent with our present data. This inconsistency is probably due to the difference in the age of mice in the present study (6 wk of age) from the ages of the mice that Reimann et al. (21) studied (~11–14.5 mo of age).

In the *mdx* mice, we found no significant correlation between muscle damage and expression level of *pax7* (Fig. 3*C*) and no correlation between muscle damage and the ratio of satellite cells to the total number of cell nuclei in the muscle tissues (Fig. 4*F*), suggesting that the levels of activation and proliferation of muscle satellite cells are not correlated with the degree of damage in *mdx* skeletal muscles. However, because the correlation between muscle damage and the ratio of satellite cells to the total number of cell nuclei in the muscle tissues was nearly significant (when the t value for the correlation is >2.07, the correlation is statistically significant; the t value in the present study was 2.01), muscle satellite cells seem to be one of several factors influencing the degree of damage in *mdx* skeletal muscles, but not a great influencing factor. Gillis (12) proposed the following three factors that can lead to severe myofiber damage in the *mdx* diaphragm muscle: a large proportion of fast oxidative fibers having a large diameter, lifelong sustained activity, and forced lengthening during each contraction. Further studies are necessary to elucidate the factors that determine the degree of damage in *mdx* skeletal muscles other than the diaphragm muscle.

In both the B10 and *mdx* mice, the ratios of m-cadherin-positive cells to the total number of cell nuclei in the muscle tissues were greatest in the masseter muscles. This result indicates that the masseter muscle contains the largest pool of satellite cells, suggesting that the regeneration potential of the masseter muscle is much larger than that of the other muscles. If the same situation existed in the *mdx* muscles before the first episode of degeneration, it would not be surprising for the *mdx* masseter muscle to show much less damage than the *mdx* diaphragm muscle (Fig. 2*E*). In the present study, however, a clear and statistically significant negative correlation between muscle damage and the percentage of satellite cells could not be obtained (Fig. 4*F*). This result is probably due to the existence of other factors more influential than satellite cells. Masseter muscle reportedly has several unique characteristics (3, 5, 17, 26, 28, 32), and to these we may now add the characteristic of having a large pool of satellite cells and a large potential for regeneration.

Previous studies have reported that utrophin can functionally replace dystrophin and that the transgene expression of utrophin can prevent muscular dystrophy in *mdx* mice (2, 7, 30). Thus we had expected a high negative correlation between damage to the skeletal muscles and the expression level of utrophin mRNA in the *mdx* mice. Contrary to our expectation, the correlation coefficient between muscle damage and expression level was low and not significantly different from zero (Fig. 5*B*). In particular, the *mdx* diaphragm muscle exhibited the highest expression level for utrophin mRNA, although it was the most severely damaged by dystrophy. To determine whether upregulated utrophin cannot functionally replace dystrophin because it is not incorporated into the sarcolemma instead of dystrophin, we investigated the immunolocalization of utrophin (Fig. 5, *C–F*). Because intense immunostaining for utrophin was observed in the periphery of *mdx* myofibers (Fig. 5, *D* and *F*), we presumed that it was incorporated into the sarcolemma. In the present study, the expression level of utrophin mRNA in the *mdx* diaphragm muscle was ~1.4- to 2.7-fold the levels in the other three *mdx* muscles studied (Fig. 5*A*). To obtain complete disappearance of muscle damage, transgene expression is needed to reach ~11- and 25-fold the utrophin expression in *mdx* and normal mice, respectively (22). Thus it is most likely that the difference in the spontaneous upregulation of utrophin among different *mdx* muscles is too small to produce a difference in the degree of damage among different *mdx* muscles.

ACKNOWLEDGMENTS

We thank M. Chiba, Tsurumi University School of Dental Medicine, for support throughout the present study.

GRANTS

This study was supported in part by Grants-in-Aid for Funding Scientific Research 13671955 and 16591871 (to A. Yamane); the Bio-ventures and High-Technology Research Center from the Ministry of Education, Culture, Sports, Science, and Technology of Japan; and the Science Research Promotion Fund from the Promotion and Mutual Aid Corporation for Private Schools of Japan.

REFERENCES

1. **Adams GR.** Role of insulin-like growth factor-I in the regulation of skeletal muscle adaptation to increased loading. *Exerc Sport Sci Rev* 26: 31–60, 1998.
2. **Blake DJ, Weir A, Newey SE, and Davies KE.** Function and genetics of dystrophin and dystrophin-related proteins in muscle. *Physiol Rev* 82: 291–329, 2002.
3. **Butler-Browne GS, Eriksson PO, Laurent C, and Thornell LE.** Adult human masseter muscle fibers express myosin isozymes characteristic of development. *Muscle Nerve* 11: 610–620, 1988.
4. **Chargé SBP and Rudnicki MA.** Cellular and molecular regulation of muscle regeneration. *Physiol Rev* 84: 209–238, 2004.
5. **D'Albis A, Janmot C, and Bechet JJ.** Comparison of myosins from the masseter muscle of adult rat, mouse and guinea-pig: persistence of neonatal-type isoforms in the murine muscle. *Eur J Biochem* 156: 291–296, 1986.
6. **Deconinck AE, Rafael JA, Skinner JA, Brown SC, Potter AC, Metzinger L, Watt DJ, Dickson JG, Tinsley JM, and Davies KE.** Utrophin-dystrophin-deficient mice as a model for Duchenne muscular dystrophy. *Cell* 90: 717–727, 1997.
7. **Deconinck N, Tinsley J, De Backer F, Fisher R, Kahn D, Phelps S, Davies K, and Gillis JM.** Expression of truncated utrophin leads to major functional improvements in dystrophin-deficient muscles of mice. *Nat Med* 3: 1216–1221, 1997.
8. **De la Porte S, Morin S, and Koenig J.** Characteristics of skeletal muscle in mdx mutant mice. *Int Rev Cytol* 191: 99–148, 1999.
9. **Dixon AK, Tait TM, Campbell EA, Bobrow M, Roberts RG, and Freeman TC.** Expression of the dystrophin-related protein 2 (*Drp2*) transcript in the mouse. *J Mol Biol* 270: 551–558, 1997.
10. **Dupont-Versteegden EE and McCarter RJ.** Differential expression of muscular dystrophy in diaphragm versus hindlimb muscles of mdx mice. *Muscle Nerve* 15: 1105–1110, 1992.
11. **Gilliland G, Perrin S, Blanchard K, and Bunn HF.** Analysis of cytokine mRNA and DNA: detection and quantitation by competitive polymerase chain reaction. *Proc Natl Acad Sci USA* 87: 2725–2729, 1990.

12. **Gillis JM.** The mdx mouse diaphragm: exercise-induced injury. *Muscle Nerve* 20: 394, 1997.
13. **Hawke TJ and Garry DJ.** Myogenic satellite cells: physiology to molecular biology. *J Appl Physiol* 91: 534–551, 2001.
14. **Hill M and Goldspink G.** Expression and splicing of the insulin-like growth factor gene in rodent muscle is associated with muscle satellite (stem) cell activation following local tissue damage. *J Physiol* 549: 409–418, 2003.
15. **Irintchev A, Zeschnigk M, Starzinski-Powitz A, and Wernig A.** Expression pattern of M-cadherin in normal, denervated, and regenerating mouse muscles. *Dev Dyn* 199: 326–337, 1994.
16. **Muller J, Vayssiere N, Royuela M, Leger ME, Muller A, Bacou F, Pons F, Hugon G, and Mornet D.** Comparative evolution of muscular dystrophy in diaphragm, gastrocnemius and masseter muscles from old male mdx mice. *J Muscle Res Cell Motil* 22: 133–139, 2001.
17. **Noden DM, Marcucio R, Borycki AG, and Emerson CP Jr.** Differentiation of avian craniofacial muscles: I. patterns of early regulatory gene expression and myosin heavy chain synthesis. *Dev Dyn* 216: 96–112, 1999.
18. **Ohnuki Y, Saeki Y, Yamane A, and Yanagisawa K.** Quantitative changes in the mRNA for contractile proteins and metabolic enzymes in masseter muscle of bite-opened rats. *Arch Oral Biol* 45: 1025–1032, 2000.
19. **Padilla F, Mège RM, Sobel A, and Nicolet M.** Upregulation and redistribution of cadherins reveal specific glial and muscle cell phenotypes during Wallerian degeneration and muscle denervation in the mouse. *J Neurosci Res* 58: 270–283, 1999.
20. **Porter JD, Rafael JA, Ragusa RJ, Brueckner JK, Trickett JI, and Davies KE.** The sparing of extraocular muscle in dystrophinopathy is lost in mice lacking utrophin and dystrophin. *J Cell Sci* 111: 1801–1811, 1998.
21. **Reimann J, Irintchev A, and Wernig A.** Regenerative capacity and the number of satellite cells in soleus muscles of normal and mdx mice. *Neuromuscul Disord* 10: 276–282, 2000.
22. **Rybakova IN, Patel JR, Davies KE, Yurchenco PD, and Ervasti JM.** Utrophin binds laterally along actin filaments and can couple costameric actin with sarcolemma when overexpressed in dystrophin-deficient muscle. *Mol Biol Cell* 13: 1512–1521, 2002.
23. **Sabourin LA and Rudnicki MA.** The molecular regulation of myogenesis. *Clin Genet* 57: 16–25, 2000.
24. **Seale P, Sabourin LA, Girgis-Gabardo A, Mansouri A, Gruss P, and Rudnicki MA.** Pax7 is required for the specification of myogenic satellite cells. *Cell* 102: 777–786, 2000.
25. **Siebert PD and Larrick JW.** Competitive PCR. *Nature* 359: 557–558, 1992.
26. **Soussi-Yanicostas N, Barbet JP, Laurent-Winter C, Barton P, and Butler-Browne GS.** Transition of myosin isozymes during development of human masseter muscle: persistence of developmental isoforms during postnatal stage. *Development* 108: 239–249, 1990.
27. **Stedman HH, Sweeney HL, Shrager JB, Maguire HC, Panettieri RA, Petrof B, Narusawa M, Leferovich JM, Sladky JT, and Kelly AM.** The mdx mouse diaphragm reproduces the degenerative changes of Duchenne muscular dystrophy. *Nature* 352: 536–539, 1991.
28. **Tajbakhsh S, Rocancourt D, Cossu G, and Buckingham M.** Redefining the genetic hierarchies controlling skeletal myogenesis: *Pax-3* and *Myf-5* act upstream of *MyoD*. *Cell* 89: 127–138, 1997.
29. **Tiffin N, Williams RD, Shipley J, and Pritchard-Jones K.** *PAX7* expression in embryonal rhabdomyosarcoma suggests an origin in muscle satellite cells. *Br J Cancer* 89: 327–332, 2003.
30. **Tinsley J, Deconinck N, Fisher R, Kahn D, Phelps S, Gillis JM, and Davies K.** Expression of full-length utrophin prevents muscular dystrophy in mdx mice. *Nat Med* 4: 1441–1444, 1998.
31. **Urushiyama T, Akutsu S, Miyazaki JI, Fukui T, Diekwisch TGH, and Yamane A.** Change from a hard to soft diet alters the expression of insulin-like growth factors, their receptors, and binding proteins in association with atrophy in adult mouse masseter muscle. *Cell Tissue Res* 315: 97–105, 2004.
32. **Wachtler F and Christ B.** The basic embryology of skeletal muscle formation in vertebrates: the avian model. *Semin Dev Biol* 3: 217–227, 1992.
33. **Weir AP, Burton EA, Harrod G, and Davies KE.** A- and B-utrophin have different expression patterns and are differentially up-regulated in *mdx* muscle. *J Biol Chem* 277: 45285–45290, 2002.
34. **Yamane A, Mayo M, Shuler C, Crowe D, Ohnuki Y, Dalrymple K, and Saeki Y.** Expression of myogenic regulatory factors during the development of mouse tongue striated muscle. *Arch Oral Biol* 45: 71–78, 2000.
35. **Yamane A, Mayo ML, and Shuler C.** The expression of insulin-like growth factor-I, II and their cognate receptor 1 and 2 during mouse tongue embryonic and neonatal development. *Zool Sci* 17: 935–945, 2000.
36. **Yamane A, Takahashi K, Mayo M, Vo H, Shum L, Zeichner-David M, and Slavkin HC.** Induced expression of MyoD, myogenin and desmin during myoblast differentiation in embryonic mouse tongue development. *Arch Oral Biol* 43: 407–416, 1998.

Volume ■(■): 1–10, 2006
Journal of Histochemistry & Cytochemistry
http://www.jhc.org

ARTICLE

Sphingomyelin Levels in the Plasma Membrane Correlate with the Activation State of Muscle Satellite Cells

Yosuke Nagata, Hideshi Kobayashi, Masato Umeda, Naoshi Ohta, Seiichiro Kawashima, Peter S. Zammit, and Ryoichi Matsuda

Department of Life Sciences, The University of Tokyo, Tokyo, Japan (YN,RM); Muscle Cell Biology Group, Medical Research Council Clinical Sciences Centre, Imperial College, London, United Kingdom (YN,PSZ); Randall Division of Cell and Molecular Biophysics, King's College London School of Biomedical and Health Sciences, Guy's Campus, London, United Kingdom (PSZ); Department of Molecular Biodynamics, The Tokyo Metropolitan Institute of Medical Science, Tokyo, Japan (HK,MU); Research Laboratory, Zenyaku Kogyo Co. Ltd., Tokyo, Japan (NO,SK)

SUMMARY Satellite cells are responsible for postnatal growth, hypertrophy, and regeneration of skeletal muscle. They are normally quiescent, and must be activated to fulfill these functions, yet little is known of how this is regulated. As a first step in determining the role of lipids in this process, we examined the dynamics of sphingomyelin in the plasma membrane. Sphingomyelin contributes to caveolae/lipid rafts, which act to concentrate signaling molecules and are also precursors of several bioactive lipids. Proliferating or differentiated C2C12 muscle cells did not bind lysenin, a sphingomyelin-specific binding protein, but noncycling reserve cells did. Quiescent satellite cells also bound lysenin, revealing high levels of sphingomyelin in their plasma membranes. On activation, however, the levels of sphingomyelin drop, so that lysenin did not label proliferating satellite cells. Although most satellite cell progeny differentiate, others stop cycling, maintain Pax7, downregulate MyoD, and escape immediate differentiation. Importantly, many of these Pax7+ve/MyoD-ve cells also regained lysenin binding on their surface, showing that the levels of sphingomyelin had again increased. Our observations show that quiescent satellite cells are characterized by high levels of sphingomyelin in their plasma membranes and that lysenin provides a novel marker of myogenic quiescence. (J Histochem Cytochem ■:1–10, 2006)

KEY WORDS
satellite cell
stem cell
skeletal muscle
activation
regeneration
sphingolipid
sphingomyelin
lysenin

SKELETAL MUSCLE CONTAINS both differentiated myofibers and stem cells, termed satellite cells. Myofibers are long, multinucleated cells specialized for rapid force generation. Muscle satellite cells are mononucleated and closely associated with myofibers, being located within the basal lamina that surrounds each myofiber (Mauro 1961). Satellite cells are responsible for postnatal growth, hypertrophy, and repair of skeletal muscle [reviewed in Zammit and Beauchamp (2001)]. In adult muscle, satellite cells are mitotically quiescent (Schultz et al. 1978), but can be activated to enter the cell cycle and produce myogenic precursor cells that then differentiate and fuse into multinucleated myotubes or existing myofibers (Snow 1977,1978). The numbers and replicative capacity of satellite cells are severely reduced in myopathic conditions such as Duchenne muscular dystrophy (Schultz and Jaryszak 1985; Webster and Blau 1990) showing the importance of regulated satellite cell activation for maintaining functional skeletal muscle.

Signals released from crushed myofibers, invading macrophages, and connective tissue have been implicated in the initiation of satellite cell activation (reviewed in Charge and Rudnicki 2004). However, the molecular mechanisms responsible for the transduction of such extracellular signals in satellite cells remain poorly defined and the potential role of lipid-mediated signaling has not previously been considered in this context.

Lipids have been recognized to play vital roles in various cellular functions. For example, phosphatidyl-

Correspondence to: Dr. Ryoichi Matsuda, Department of Life Sciences, The University of Tokyo, Rm. 15-309A, 3-8-1 Komaba, Meguro-ku, Tokyo 153-8902, Japan. E-mail: cmatsuda@mail.ecc.u-tokyo.ac.jp

Received for publication March 2, 2005; accepted September 14, 2005 [DOI: 10.1369/jhc.5A6675.2006].

0022-1554/05/$3.30

serine is involved in myoblast fusion (van den Eijnde et al. 2001), and phosphatidylethanolamine is essential in cytokinesis (Emoto and Umeda 2000). Although differences in phospholipid composition during myoblast differentiation and fusion have been reported (Kent et al. 1974; Sessions and Horwitz 1983; Anderson 1991; Pediconi et al. 1992), the dynamics of phospholipid composition during satellite cell activation remains unknown.

Sphingomyelin is an integral lipid component of cell membranes in animals. Although sphingomyelin is located in intracellular membranes such as those of the endosomes, lysosomes, and Golgi apparatus and nucleus, significant amounts are also found in the plasma membrane [reviewed in van Meer and Holthuis (2000)]. Sphingomyelin in the plasma membrane forms lipid microdomains with other sphingolipids, cholesterols, and proteins. It has been suggested that these rafts or caveolae lipid microdomains facilitate cytoplasmic signaling by acting to concentrate signaling molecules [reviewed in Simons and Toomre (2000)]. Moreover, sphingomyelin in the plasma membrane also acts as a reservoir of bioactive sphingolipids. Sphingomyelin metabolites, such as ceramide, sphingosine, and sphingosine-1-phosphate, are emerging as important regulators of a variety of cellular events, including cell proliferation, differentiation, and apoptosis (reviewed in Ohanian and Ohanian 2001; Spiegel and Milstien, 2003). Despite the importance of these sphingomyelin metabolites, few studies have attempted to examine the dynamics of cellular sphingomyelin, and those that have, have relied on indirect biochemical analysis of extracted lipids lacking single-cell resolution [e.g., Kent et al. (1974)].

In this study, we focus on sphingomyelin levels in the plasma membrane of myogenic cells using lysenin, a protein isolated from the earthworm *Eisenia foetida* (Sekizawa et al. 1997; reviewed in Kobayashi et al. 2004). Because lysenin binds specifically to sphingomyelin (Yamaji et al. 1998), we used it to directly assay sphingomyelin levels in individual myogenic cells as they activate from quiescence. We initially used C2 reserve cells, which model myogenic cell quiescence (Yoshida et al. 1998). Lysenin bound selectively to quiescent reserve cells, but not cycling and differentiated cells, indicating sphingomyelin levels fell with activation. Quiescent satellite cells also had robust lysenin immunostaining, showing that sphingomyelin levels were also high on myogenic cells in vivo. During satellite cell activation and subsequent proliferation, however, sphingomyelin levels became practically undetectable. Some satellite cells maintained in culture adopt characteristics consistent with a return to a quiescent-like state (Zammit et al. 2004). Importantly, many of these cells also regained lysenin binding, showing that sphingomyelin levels in their plasma membranes had increased to levels seen in quiescent satellite cells.

Materials and Methods

Cell Culture

C2C12 myogenic cells (Yaffe and Saxel 1977; Blau et al. 1983) were maintained in growth medium comprising DMEM (Gibco; Grand Island, NY) containing 20% FBS (Equitec-Bio; Kerrville, TX), 4 mM L-glutamine, 100 U/ml penicillin, and 100 μg/ml streptomycin (Sigma; St. Louis, MO) at 37C in 5% CO_2. To induce differentiation and produce reserve cells, 5×10^4 cells were seeded on a 35-mm tissue culture dish in growth medium, and, 24 hr later, the medium was replaced with serum-free differentiation medium (DMEM supplemented with 5 μg/ml insulin, 5 μg/ml transferrin, 5 ng/ml sodium selenite, and 1 mg/ml BSA (Sigma).

To isolate reserve cells from myotubes, C2C12 cells were cultured in differentiation medium for 4–5 days and then all cells were detached using with 0.05% trypsin-0.53 mM EDTA (Gibco; Grand Island, NY) for 5 min at 37C. Cells were then plated in fresh 20% FBS/DMEM in new Petri dishes. After 30 min at 37C, cells were gently rinsed with PBS to remove floating cells (mostly myotubes) and further cultured in 20% FBS/DMEM.

Phospholipid Analysis

To determine the phospholipid content, 8×10^5 C2C12 cells were plated per 300-mm tissue culture dish in growth medium, and 24 hr later, the medium was switched to serum-free differentiation medium. Four days later, reserve cells and myotubes were separated using a modified version of the method of Kitzmann et al. (1998). Briefly, cells were rinsed with PBS containing 0.1 g/liter $MgCl_2/6H_2O$ and 0.13 g/liter $CaCl_2/2H_2O$ before incubation with 0.05% trypsin (without EDTA) at room temperature for 5–10 min. Myotubes detach under these conditions and were collected. Residual cells remained attached and were then rinsed with PBS and collected using standard trypsin-EDTA, as detailed previously. Lipids were then extracted from each fraction according to the method of Bligh and Dyer (1959) and were separated on a silica gel 60 TLC plate (Merck; Darmstadt, Germany) using chloroform/methanol/acetic acid/water (100:75:7:4, v/v). Lipids were then visualized with iodine vapor and compared with those of standards before being assayed for phosphorous content with malachite green reagent (Sigma) (Zhou and Arthur 1992).

Isolation and Culture of Mouse Myofibers

Single myofibers with associated satellite cells were prepared as previously described (Rosenblatt et al. 1995). Briefly, adult (~8 weeks old) C57BL/6 mice were killed by cervical dislocation and the extensor digitorum longus muscle was carefully removed. After washing with PBS, the muscles were immersed in 0.6% Collagenase Type I (Worthington Biochemical; Lakewood, NJ) in DMEM and incubated at 38C for 100 min with agitation. Single myofibers were then liberated from the muscle by repeatedly triturating with a Pasteur pipette and then washed in several changes of DMEM. For the analysis of quiescent satellite cells, myofibers were immediately fixed by the addition of 4% paraformaldehyde/PBS for 10 min before washing in PBS. To activate the associated satellite cells, myofibers were cultured in suspension in